

## INTRINSIC BRIGHTNESS TEMPERATURES OF AGN JETS

D. C. HOMAN,<sup>1</sup> Y. Y. KOVALEV,<sup>2,3</sup> M. L. LISTER,<sup>4</sup> E. ROS,<sup>5</sup> K. I. KELLERMANN,<sup>6</sup> M. H. COHEN,<sup>7</sup>  
 R. C. VERMEULEN,<sup>8</sup> J. A. ZENSUS,<sup>5</sup> AND M. KADLER<sup>5,9</sup>

Received 2006 February 3; accepted 2006 March 30; published 2006 April 19

### ABSTRACT

We present a new method for studying the intrinsic brightness temperatures of the parsec-scale jet cores of active galactic nuclei (AGNs). Our method uses observed superluminal motions and observed brightness temperatures for a large sample of AGNs to constrain the characteristic intrinsic brightness temperature of the sample as a whole. To study changes in intrinsic brightness temperature, we assume that the Doppler factors of individual jets are constant in time, as justified by their relatively small changes in observed flux density. We find that in their median-low brightness temperature state, the sources in our sample have a narrow range of intrinsic brightness temperatures centered on a characteristic temperature,  $T_{\text{int}} \approx 3 \times 10^{10}$  K, which is close to the value expected for equipartition, when the energy in the radiating particles equals the energy stored in the magnetic fields. However, in their maximum brightness state, we find that sources in our sample have a characteristic intrinsic brightness temperature greater than  $2 \times 10^{11}$  K, which is well in excess of the equipartition temperature. In this state, we estimate that the energy in radiating particles exceeds the energy in the magnetic field by a factor of  $\sim 10^5$ . We suggest that the excess of particle energy when sources are in their maximum brightness state is due to injection or acceleration of particles at the base of the jet. Our results suggest that the common method of estimating jet Doppler factors by using a single measurement of observed brightness temperature, the assumption of equipartition, or both may lead to large scatter or systematic errors in the derived values.

*Subject headings:* galaxies: active — galaxies: jets — galaxies: kinematics and dynamics — radiation mechanisms: nonthermal — radio continuum: galaxies

### 1. INTRODUCTION

A key physical property of extragalactic radio jets is the relationship between the energy stored in the radiating particles and the energy stored in the magnetic field. Burbidge (1959) originally suggested that these energies were approximately in balance, or equipartition, as a way of minimizing the total energy stored in extended radio lobes, and more recent work (Croston et al. 2005) has indeed shown that extended radio lobes are at or very near equipartition. However, it is still unknown whether this balance is established at, or close to, the base of the jet, or if jets begin far out of equipartition and only reach equipartition after significant periods of time.

The energy balance at the base of extragalactic radio jets can be studied by measuring the brightness temperature of jet cores using the Very Long Baseline Array (VLBA). The intrinsic brightness temperature,  $T_{\text{int}}$ , is related to the energy balance by the following expression:

$$T_{\text{int}} = \eta^{1/8.5} T_{\text{eq}} \quad (1)$$

<sup>1</sup> Department of Physics and Astronomy, Denison University, Granville, OH 43023; homand@denison.edu.

<sup>2</sup> Jansky Fellow, National Radio Astronomy Observatory, P.O. Box 2, Green Bank, WV 24944.

<sup>3</sup> Astro Space Center, P. N. Lebedev Physical Institute, ulitsa Profsoyuznaya 84/32, 117997 Moscow, Russia.

<sup>4</sup> Department of Physics, Purdue University, 525 Northwestern Avenue, West Lafayette, IN 47907.

<sup>5</sup> Max-Planck-Institut für Radioastronomie, Auf dem Hügel 69, D-53121 Bonn, Germany.

<sup>6</sup> National Radio Astronomy Observatory, 520 Edgemont Road, Charlottesville, VA 22903.

<sup>7</sup> Department of Astronomy, Mail Code 105-24, California Institute of Technology, 1200 East California Boulevard, Pasadena, CA 91125.

<sup>8</sup> Netherlands Foundation for Research in Astronomy, Postbus 2, NL-7990 AA Dwingeloo, Netherlands.

<sup>9</sup> Current address: Goddard Space Flight Center, Greenbelt, MD 20771.

(Readhead 1994), where  $\eta = u_p/u_B$  is the ratio of the energy densities of the radiating particles,  $u_p$ , to the magnetic field,  $u_B$ .  $T_{\text{eq}} \approx 5 \times 10^{10}$  K is the equipartition brightness temperature defined by Readhead (1994), and the exponent of  $\eta$  assumes a power-law Lorentz factor distribution for the radiating particles with index  $p = 2.5$  for  $N_\gamma d\gamma = K\gamma^{-p} d\gamma$ . This corresponds to a spectral index of  $\alpha = -0.75$  ( $S \propto \nu^{+\alpha}$ ) in the optically thin parts of the jet.

The intrinsic brightness temperatures of AGN cores are limited either by the inverse Compton catastrophe to be  $T_{\text{int}} \lesssim 10^{12}$  K (Kellermann & Pauliny-Toth 1969) or by the possibility that jets are near equipartition to begin with so that  $T_{\text{int}} \approx T_{\text{eq}}$  (Singal & Gopal-Krishna 1985; Singal 1986; Readhead 1994). If AGN cores are indeed limited by the inverse Compton catastrophe, they must be very far out of equipartition, with  $\eta \sim 10^{11}$  (see, e.g., Kellermann & Pauliny-Toth 1969).

Unfortunately, it is very difficult to measure intrinsic brightness temperatures because AGN jets are highly relativistic and therefore Doppler boosted. So with very long baseline interferometry (VLBI), we do not measure the  $T_{\text{int}}$  directly, but rather the observed brightness temperature<sup>10</sup>  $T_{\text{obs}} = \delta T_{\text{int}}$ , where  $\delta$  is the Doppler factor of the jet, given by

$$\delta = \frac{\sqrt{1 - \beta^2}}{1 - \beta \cos \theta}, \quad (2)$$

where  $\beta$  is the speed of the relativistic flow in units of the speed of light and  $\theta$  is the angle the jet makes with the line of

<sup>10</sup> For this Letter we take all observed brightness temperatures from the point of view of an observer comoving with the AGN host galaxy, so we have corrected for redshift. We also assume that radiation is emitted isotropically in the comoving frame, and that the parsec-scale jet cores have a flat spectrum ( $\alpha = 0$ ) due to optical depth effects. Our choice of cosmology is  $H_0 = 70 \text{ km s}^{-1} \text{ Mpc}^{-1}$ ,  $\Omega_m = 0.3$ , and  $\Omega_\Lambda = 0.7$ .

sight. The speed of the jet is often characterized by its bulk Lorentz factor,  $\Gamma = 1/(1 - \beta^2)^{1/2}$ .

Observed brightness temperatures from ground-based VLBI can range up to lower limits of  $T_{\text{obs}} \geq 5 \times 10^{13}$  K (e.g., Kovalev et al. 2005), and observed brightness temperatures in excess of  $1 \times 10^{14}$  K have been reported with space VLBI (e.g., Horiuchi et al. 2004). Horiuchi et al. (2004) find typical observed brightness temperatures in the range of  $1 \times 10^{11}$  to  $1 \times 10^{13}$  K from the 5 GHz survey of the Japanese space VLBI program VSOP, and Kovalev et al. (2005) find a similar range from ground-based VLBA measurements at 15 GHz. The recent discovery of very nearby scintillation screens has brought the maximum brightness temperatures deduced from intraday variability into the same range as those measured through VLBI, even though interstellar scintillation is potentially sensitive to much smaller angular sizes than the VLBA (Lovell et al. 2003 and references therein).

In this Letter, we present a new method for deducing the typical intrinsic brightness temperature for parsec-scale AGN cores from a population of well-studied VLBA jets. These cores represent the optically thick region at the start of the jet as seen in VLBI images. We combine observed brightness temperature data from Kovalev et al. (2005) and proper-motion data from the 2 cm VLBA survey (e.g., Kellermann et al. 2004). In § 2, we discuss the theory behind our approach, and in § 3 we present our results and discuss the implications for energy balance between particles and magnetic fields at the base of AGN jets.

## 2. METHODOLOGY

The basis of our approach is to compare the observed brightness temperatures,  $T_{\text{obs}}$ , for a collection of parsec-scale AGN jet cores with the proper motions of their jets,  $\beta_{\text{app}}$ . Proper motion,  $\beta_{\text{app}} = \beta \sin \theta / (1 - \beta \cos \theta)$ , will serve as a proxy for the jet Doppler factor,  $\delta$ , which we cannot easily measure. For the purposes of this analysis, we assume that the speeds of the fastest jet components are the same as the flow speed through the jet core. We also assume that the jets are straight, with no bends between the jet core and the location of jet components. To the degree that these assumptions are incorrect, one should expect some scatter in our final results.

To generate a simple model, we make two further assumptions: (1) that all jets in our sample have the same intrinsic brightness temperature,  $T_{\text{int}}$ , and (2) that all sources are close to the critical angle  $\theta_c = \arccos \beta$  for the maximal superluminal motion at a given  $\beta$ . Under these strict assumptions,  $\delta \approx \beta_{\text{app}}$  and  $T_{\text{obs}} \approx \beta_{\text{app}} T_{\text{int}}$ , and therefore  $\beta_{\text{app}}$  is a simple function of the observed brightness temperature, as represented by the solid line in Figure 1.

Of course, the assumption that all jets are near the critical angle is poor. For a flux-limited sample, the majority will lie inside the critical angle, where the Doppler factor exceeds the Lorentz factor (Vermeulen & Cohen 1994). The probability distribution for jet orientations in a beamed, flux-limited sample has been studied in detail by Vermeulen & Cohen (1994) and Lister & Marscher (1997). In Figure 1,  $\beta_{\text{app}}$  is plotted versus  $T_{\text{obs}}$  from a numerical simulation of a flux-limited sample of 1000 AGN jets. This simulation is based on Lister & Marscher (1997) and assumes that all jets have the same intrinsic brightness temperature  $T_{\text{int}} = 5 \times 10^{10}$  K. The jet speeds in the population range from  $\beta = 0.05$  to  $\Gamma = 30$  and are distributed according to  $n(\Gamma) \propto \Gamma^{-1.5}$ . These simulated jets are drawn from

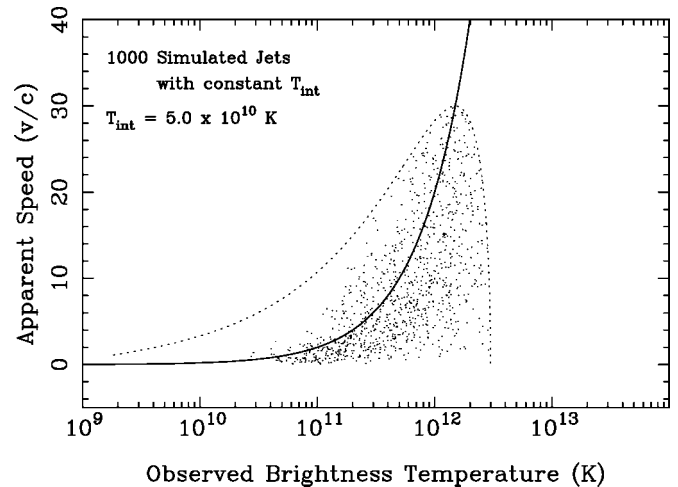


FIG. 1.—Plot of 1000 fictional sources from a program that simulates a relativistically beamed population of AGN jets selected on the basis of observed flux. All sources are given the same intrinsic brightness temperature. The solid line represents where sources observed at the critical angle would lie on this plot. The dashed line represents the possible apparent speeds of a  $\Gamma = 30$  source with intrinsic brightness temperature given by  $T_{\text{int}}$ .

a randomly oriented parent population with an intrinsic (unbeamed) luminosity function consistent with that of the FR II radio galaxies described in Lister & Marscher (1997). The luminosity function has a lower cutoff at  $1 \times 10^{23}$  W Hz $^{-1}$  and incorporates pure exponential luminosity evolution while maintaining a constant comoving space density out to  $z = 4$ .

Approximately 75% of the sources in Figure 1 fall below and to the right of the solid line, representing the critical angle; these sources are inside the critical angle, and while they have large Doppler factors, many of them are close enough to the line of sight to have small proper motions. The dotted line in Figure 1 shows the apparent speed for a jet with the maximal Lorentz factor of  $\Gamma = 30$  in the simulation as a function of  $T_{\text{obs}}$ , corresponding to a varying jet viewing angle. The dotted line, therefore, represents an upper envelope for the simulation.

The scatter in Figure 1 gives a realistic idea of what we might expect for a “best case” correlation between  $\beta_{\text{app}}$  and  $T_{\text{obs}}$  for real data under the assumptions that jets are straight, pattern speeds are the same as flow speeds, and all jets have the same  $T_{\text{int}}$ . However, even with the scatter induced by selection effects, the trend is clear, particularly the lack of sources with *both* low observed brightness temperature *and* fast proper motion.

## 3. RESULTS AND DISCUSSION

We have collected multiepoch brightness temperature measurements for 106 sources that all have well-studied proper motions and at least five epochs of brightness temperature measurements. The brightness temperature measurements are taken from Kovalev et al. (2005), and the proper-motion measurements are updated from Kellermann et al. (2004) to include additional epochs from the VLBA<sup>11</sup> 2 cm survey<sup>12</sup> through 2002 (E. Ros et al. 2006, in preparation). As described in Kellermann et al. (2004), we use the fastest proper motion for each source, and we only consider those motions that are ranked as “ex-

<sup>11</sup> The Very Long Baseline Array is operated by the National Radio Astronomy Observatory, a facility of the National Science Foundation operated under cooperative agreement by Associated Universities, Inc.

<sup>12</sup> See <http://www.cv.nrao.edu/2cmsurvey>.

cellent” (E) or “good” (G) by the criteria laid out in that paper. Of the 106 sources plotted here, 70 are members of the 133-source, flux-limited MOJAVE<sup>13</sup> sample (Lister & Homan 2005). The remaining 36 sources are members of the 2 cm survey but do not meet the selection criteria of the MOJAVE program.

Figure 2 is a three-panel plot of  $\beta_{\text{app}}$  versus  $T_{\text{obs}}$ . Figure 2a contains 106 fictional sources from the simulation plotted in Figure 1. The 106 fictional sources are selected in a manner analogous to our actual data, with 70 of them chosen at random from the 133 brightest sources in the simulation and the remaining 36 chosen at random from the rest. This panel is included to illustrate that selection criteria similar to our real sample will still produce a plot very similar to Figure 1, with about 75% of the points falling below and to the right of the solid line representing sources at the critical angle. As in Figure 1, the dotted line in each panel is the apparent speed for a jet with a bulk Lorentz factor of 30 as a function of  $\theta$ . If all sources had the same  $T_{\text{int}}$  and none had  $\Gamma > 30$ , the dotted line would encompass all of the sources.

Figure 2b is a plot of  $\beta_{\text{app}}$  versus the maximum observed brightness temperature for each source in our real sample. The solid line represents sources at the critical angle that have  $T_{\text{int}} = 2 \times 10^{11}$  K, and the same value for  $T_{\text{int}}$  is used in calculating the dotted “envelope.” This value of  $T_{\text{int}}$  was chosen so that approximately 75% of the sources would fall below and to the right of the solid line, thus matching our expectation from the simulation. Figure 2c is a similar plot except that it shows sources in their median-low state, what we call the “25% median.” This is the median of the lowest half of the brightness temperature observations for a given source. In this way, the 25% median represents a typical low brightness state for each source. The  $\approx 75\%$  line for the 25% median values is  $T_{\text{int}} = 3 \times 10^{10}$  K. A more detailed fit of our data to the distribution of simulation points in Figure 2a is beyond the scope of this Letter, and we note that other reasonable choices for the simulation parameters described in § 2 will give a roughly similar distribution of points and are likely to yield fractions between 60% and 80% of sources within the critical angle. For a 60% fraction, we would have deduced  $T_{\text{int}} = 3 \times 10^{11}$  K for the maximum case and  $T_{\text{int}} = 4 \times 10^{10}$  K for the median-low case.

It is interesting that plotting  $\beta_{\text{app}}$  versus  $T_{\text{obs}}$  in Figures 2b and 2c produces a trend very similar to that seen in the simulation, although with more scatter. There is clearly a lack of sources with *both* low observed brightness temperature *and* fast proper motion. The fact that the trend is still clear here implies that both plots are described by a narrow range of intrinsic brightness temperature, centered on the value chosen for the solid line in each plot. If the scatter in the 25% median and the maximum plots is due to intrinsic brightness temperature alone, we estimate that the real range of intrinsic brightness temperature in each case extends down to about 50% of the  $T_{\text{int}}$  for the plotted line and up to about twice this value. Note that this means the intrinsic brightness temperature ranges for the 25% median and the maximum cases do not overlap. Real sources appear to be in a distinctly different state when they display their maximum brightness temperatures.

We note that the apparent increase in brightness temperature between the 25% median and maximum states cannot be attributed to changes in the jet Doppler factors, which we have assumed to be constant in time, because the necessary large

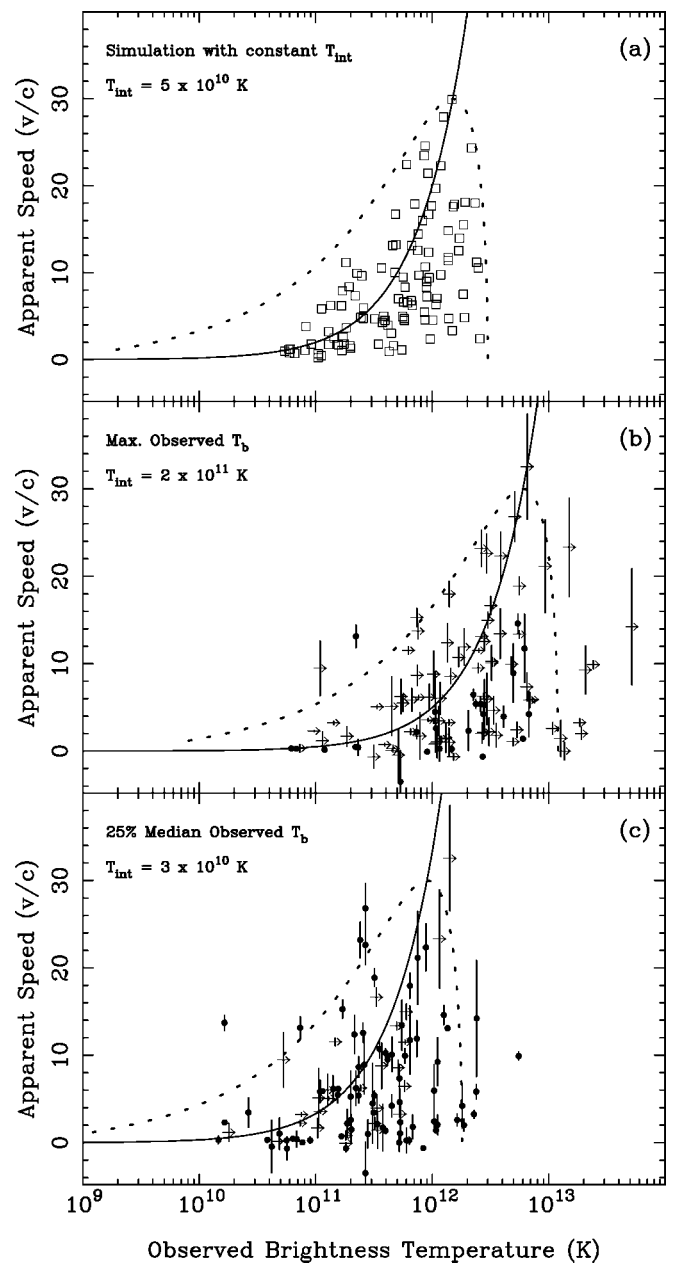


FIG. 2.—Plots of apparent motion vs. observed brightness temperature. As described in the text, (a) contains 106 sources from the simulation illustrated in Fig. 1, chosen to simulate the selection characteristics of our real data; (b) and (c) plot our real data. Lower limits are indicated by arrows and circles represent measurements. The solid lines represent sources observed at the critical angle that have the intrinsic brightness temperature indicated at upper left of each panel. The dashed lines represent the possible apparent speeds of a  $\Gamma = 30$  source with intrinsic brightness temperature given by  $T_{\text{int}}$ .

changes in Doppler factor would produce much larger changes in the flux densities of the jet cores ( $\propto \delta^2$ ), which are not observed.

The maximum plot contains more lower limits than measurements, so the characteristic value of  $T_{\text{int}}$  should really be taken as a lower limit on the characteristic value. Therefore,  $T_{\text{int}} > 2 \times 10^{11}$  K when sources display their maximum brightness temperature. From equation (1), this requires sources in that state to be well out of equipartition, with  $\eta \sim 10^5$  or greater. On the other hand, the characteristic value for the median-low state is much closer to the equipartition brightness temperature

<sup>13</sup> See <http://www.physics.purdue.edu/astro/MOJAVE>.

defined by Readhead (1994), and there are far fewer limits in that plot,<sup>14</sup> so it seems reasonable to take the characteristic median-low intrinsic brightness temperature to be  $T_{\text{int}} \approx 3 \times 10^{10}$  K.

Our data indicate that AGN jet cores are indeed near equipartition in their median-low state; however, they go well out of equipartition in their maximum brightness temperature state. In their maximum state, they have  $\geq 10^5$  times the energy in their radiating particles as they have in the magnetic fields. Such a large imbalance may be the result of injection or acceleration of particles at the base of the jet, resulting in a transient state that is in excess of the equilibrium equipartition brightness temperature. For  $\eta \sim 10^5$ , equation (5) of Readhead (1994) predicts a particle number density which has increased by a factor of 400 and a magnetic field strength that has decreased by a factor of 15 compared with the equilibrium value. We emphasize that these values are only approximate, as the precise balance between particle and field energy is a sensitive function of brightness temperature (see eq. [1]). What is robust is that the jets in our sample have a narrow range of intrinsic brightness temperatures in their median-low state, and the brightness temperatures in their maximum state are nearly an order of magnitude (or more) larger, indicating a much higher particle-to-field energy ratio.

<sup>14</sup> We note that we tried to examine the pure median case, as representative of the average state of a source; however, even the pure median case had a large number of limits (about half), and we were therefore not able to do a robust comparison with the maximum case. The 75% line for the pure median case was at  $6 \times 10^{10}$  K.

It is interesting to note that the narrow range of intrinsic brightness temperatures when sources are in their median-low state means we can derive Doppler factors for most sources that are good to a factor of 2 or better by assuming  $T_{\text{int}} = 3 \times 10^{10}$  K for the 25% median observed value. Then  $\delta = T_{\text{obs}(25\% \text{ median})} / (3 \times 10^{10} \text{ K})$ . This is very similar to the equipartition Doppler factor suggested by Singal & Gopal-Krishna (1985) and Readhead (1994); however, by using the 25% median observed brightness temperature, we obtain a much more reliable estimate for the Doppler factor. Doppler factors derived from single-epoch brightness temperature measurements (e.g., Zensus et al. 2002) are likely to have a large degree of scatter, as it is clear from this work that the intrinsic brightness temperatures of sources can vary by an order of magnitude or more. In addition, Doppler factors derived from outburst events (e.g., Lähteenmäki & Valtaoja 1999) are likely to be systematically overestimated if it is assumed that sources are near equipartition during these events.

We thank the anonymous referee for helping us to clarify several important points, and A. Lobanov for helpful discussions. This research was supported by an award from Research Corporation and NSF grant AST 04-06923. J. A. Z. acknowledges support from the Max Planck Research Award for International Research Collaboration. M. K. was supported through a stipend from the International Max Planck Research School for Radio and Infrared Astronomy at the University of Bonn.

#### REFERENCES

- Burbidge, G. R. 1959, *ApJ*, 129, 849  
 Croston, J. H., Hardcastle, M. J., Harris, D. E., Belsole, E., Birkinshaw, M., & Worrall, D. M. 2005, *ApJ*, 626, 733  
 Horiuchi, S., et al. 2004, *ApJ*, 616, 110  
 Kellermann, K. I., & Pauliny-Toth, I. I. K. 1969, *ApJ*, 155, L71  
 Kellermann, K. I., et al. 2004, *ApJ*, 609, 539  
 Kovalev, Y. Y., et al. 2005, *AJ*, 130, 2473 (erratum 131, 2361 [2006])  
 Lähteenmäki, A., & Valtaoja, E. 1999, *ApJ*, 521, 493  
 Lister, M. L., & Homan, D. C. 2005, *AJ*, 130, 1389  
 Lister, M. L., & Marscher, A. P. 1997, *ApJ*, 476, 572  
 Lovell, J. E. J., Jauncey, D. L., Bignall, H. E., Kedziora-Chudczer, L., Macquart, J.-P., Rickett, B. J., & Tzioumis, A. K. 2003, *AJ*, 126, 1699  
 Readhead, A. C. S. 1994, *ApJ*, 426, 51  
 Singal, A. K. 1986, *A&A*, 155, 242  
 Singal, K. A., & Gopal-Krishna. 1985, *MNRAS*, 215, 383  
 Vermeulen, R. C., & Cohen, M. H. 1994, *ApJ*, 430, 467  
 Zensus, J. A., Ros, E., Kellermann, K. I., Cohen, M. H., Vermeulen, R. C., & Kadler, M. 2002, *AJ*, 124, 662